applied sciences

MDPI

Article

Configurational Design of a Hybrid System Based on an Air–Water Heat Pump and Biomass Boiler for a Rural Dwelling

Javier Uche *, Milad Tajik Jamalabad and Amaya Martínez

Institute of Energy and Resources Efficiency of Aragón (ENERGAIA), University of Zaragoza, 50018 Zaragoza, Spain; mtajikjamalabad@unizar.es (M.T.J.); amayamg@unizar.es (A.M.)
* Correspondence: javiuche@unizar.es; Tel.: +34-976-762584

Abstract: Hybrid energy systems combine multiple energy sources and storage technologies to enhance performance and meet diverse energy needs. Hybrid heat pump systems are particularly suitable for heating and cooling buildings in rural areas. Air-source heat pumps have two well-known disadvantages during the coldest period of the year, when the building's heating load is at its peak: the heat pump's capacity is reduced and it needs to perform defrost cycles. A potential solution is to size the heat pump to cover only a portion of the peak load and to use a second heat generator in a hybrid heat pump system. There is a gap in the literature regarding the configurational analysis of hybrid heat pump (HHP) systems, particularly in terms of combining heat pumps and biomass boilers, and evaluating their efficiency, economic aspects, and environmental impact. Thus, in this research, a dynamic model of a HHP system, consisting of an air-to-water heat pump paired with a biomass boiler as a backup, is presented. Various configurations of the HHP system have been developed to evaluate key performance indicators, such as efficiency, emissions, operational costs, and other relevant factors. The findings of this paper indicate that the energy performance of HHP systems is significantly affected by the system layout, heat pump size, cut-off temperature, and the control algorithm used to activate the heat generators. Moreover, series operation of HHP systems is not only more efficient than parallel operation but also results in lower emissions and reduced operation costs. As expected, the energy loss associated with defrost cycles significantly impacts the overall performance of a hybrid system based on an air-source heat pump. Finally, the impact of the cut-off temperature on the key parameters in the configuration analysis was examined, and the optimal performance of the HHP system, in terms of minimizing operational costs and emissions, was depicted using a heat map diagram.

Keywords: hybrid heat pump system; configurational analysis; biomass boiler; control strategy; dynamic modeling

Citation: Uche, J.; Tajik Jamalabad, M.; Martínez, A. Configurational Design of a Hybrid System Based on an Air–Water Heat Pump and Biomass Boiler for a Rural Dwelling. *Appl. Sci.* **2024**, *14*, 9840. https://doi.org/10.3390/app14219840

Academic Editor: Satoru Okamoto

Received: 18 September 2024
Revised: 10 October 2024
Accepted: 22 October 2024
Published: 28 October 2024

1. Introduction

It is now well established that the building sector significantly contributes to the primary energy demand and greenhouse gas (GHG) emissions in developed countries [1]. With the operation of buildings accounting for 28% of global CO_2 emissions [2], alternative low-carbon technologies are necessary to meet buildings' heating and cooling needs. Reducing buildings' energy consumption and utilizing renewable energies are essential steps for decreasing greenhouse gas emissions. To enhance the efficiency of building heating and cooling systems, various solutions can be implemented [3–5]. The use of heat pumps is certainly a crucial measure to achieve energy savings.

Heat pump designs, commonly used for space cooling or heating, efficiently transfer heat from the surrounding air (or other renewable sources) to the water, rather than using energy primarily to heat water directly. Consequently, integrating a heat pump design with a backup heater can significantly increase overall efficiency, depending on the choice of heat pump technologies. Hybrid heat pumps (HHPs) combine an electrically driven heat

pump, typically an air-to-water system, with a gas condensing boiler within a single unit. Under suitable operating conditions, HHPs have been shown to achieve higher seasonal performance compared to electric-only heat pumps (EHPs). This improved performance results from the ability to operate in gas boiler (GB) mode under conditions where the EHP efficiency is lower [6]. For instance, during the coldest weather periods, when heating loads are higher and EHP performance declines, HHPs can switch to GB mode, which may be more efficient under these conditions. Moreover, since a hybrid heat pump includes a gas boiler that can be used to meet peaks in thermal demand, it allows for a lower rating of the EHP, leading to smaller EHP equipment and reduced power demand [7]. As noted by Xu [8], hybrid heating systems incorporate multiple heat sources, each fulfilling energy needs under varying time periods or operational conditions. The choice of heat sources must consider local climate and policy factors. Traditionally, boilers are preferred by investors among conventional heat sources. Importantly, there are numerous instances where a combination of electric heat pumps (HPs) and gas boiler systems is implemented on a larger scale, such as in district or industrial settings [9]. Hybrid heat pumps (HHPs) can alternate between using biomass (BM), electricity, or both (HP and boiler) to fulfill heating requirements, depending on various factors affecting system efficiency. These factors include outdoor temperature, flow temperature, and the cost of gas and electricity at any given time [10] which can make it more or less favorable to use these systems and to control them according to different strategies. A study by Dongellini et al. [11] found that over-sizing heat pumps is a critical design issue that significantly impacts the energy performance of heat pump systems, affecting both seasonal and annual energy performance. Park et al. [12] conducted an economic analysis of a hybrid heat pump system, comparing it with conventional gas-fired water heaters for residential houses in Korea. The study found that operating the hybrid system could save approximately 4% in annual energy costs. Typically, the performance of HHP systems is strongly influenced by how the hybrid system is integrated, controlled, and operated. Chargui and Sammouda [13] noted that electricity and natural gas prices play a significant role in HHP performance, as these prices can vary by region. The authors found that HHP systems are more effective in residential buildings when the system is carefully integrated to optimize both gas and electricity usage. Therefore, an effective operation strategy is crucial for a hybrid heating system.

Bellos et al. [14] investigated a configuration for both heating and cooling in buildings, utilizing a biomass-powered absorption heat pump operated with a LiBr/H2O working substance. The heating and cooling demands throughout the entire year were met by a dual-purpose biomass-driven heat pump, occasionally supplemented by a biomass boiler. The study examined the energy, economic, and environmental benefits of the proposed design. Li [15] proposed an innovative economic-based control logic for a parallel loop hybrid system consisting of an air-to-water heat pump (AWHP) and a gas-fired water heater. This control logic allows the optimal working point of the system (including the mass flow rate and supply water set-point temperature for each device) to be determined. By using this approach, significant economic benefits of up to 60% can be achieved compared to traditional solutions. Another critical factor for maximizing the energy savings attainable with the adoption of HHP systems is the sizing of the heating system components (such as the boiler, heat pump, and thermal storage) and its impact on the control system algorithm determining when to activate or deactivate the heaters. Keogh et al. [16] aimed to assess the applicability of a compact hybrid heat pump (HHP) as a retrofit solution for an Irish bungalow. The system utilized in the study was a commercially available HHP comprising an 8 kW air-source heat pump (ASHP) and a 33 kW gas boiler. They found that hybrid systems achieve greater primary energy savings compared to all-electric heat pumps because hybrid systems can adjust delivery temperatures flexibly, whereas all-electric heat pump systems typically operate with a fixed delivery temperature. Bagarella et al. [17] conducted an analysis using dynamic simulations to investigate how the control system of heaters in a hybrid system (comprising a heat pump and gas boiler) influences the seasonal efficiency of the system. They utilized numerical results to determine the optimal

values of control settings for HHP systems. Bennet et al. [18] explored the implications of hybrid heating on the residential heating sector, comparing it to both traditional technology (gas boilers) and advanced low-carbon technology (heat pumps). They discovered that a compact hybrid system featuring a 2.5 kW heat pump could potentially achieve a 50% reduction in energy demand at the national stock level. Fischer et al. [19] investigated the optimal sizing of the main elements in a hybrid system, including PV panels, air-source heat pump, electric boiler, and thermal storage. They considered factors such as electricity price, space heating load profiles, domestic hot water demand, and the size of the photovoltaic field. Their results revealed that the thermal load profile has the most significant influence on system sizing. Furthermore, Di Perna et al. [20] compared the energy performance of monovalent and bivalent heating systems, examining various types of heat generators (such as oil and gas boilers, micro CHP, and heat pumps) along with backup units (including electric heaters and gas boilers). Their findings indicated that electrical backup systems are not a financially advantageous solution.

In research conducted by Sun et al. [21], multiple buildings in Great Britain, each fitted with a hybrid heating system comprising a gas boiler and a heat pump, were examined. The study investigated the performance of these systems when operated based on electricity price variations. The results indicated that running the heat pump primarily during periods of low electricity prices and the gas boiler during peak electricity price times can lead to a 5–10% increase in the coefficient of performance (COP). D'Ettorre et al. [22] analyzed the cost-optimal sizing and hourly control strategy of a hybrid heat pump system for heating applications. Thermal storage is employed to reduce both operating costs and primary energy consumption by scheduling the operation of the heat pump during periods when energy costs are lower, thereby optimizing profitability. The findings indicated an energy cost reduction of up to 8% compared to a baseline scenario lacking storage capacity. The integration of a hybrid system with active thermal storage proves to be an effective solution for demand-side management. Martínez-Gracia et al. [23] conducted an exergy and exergy cost analysis of a solar-assisted heat pump with seasonal storage to provide electricity, heat, and domestic hot water (DHW) for social housing. They found that the monthly exergy efficiency of the photovoltaic–thermal (PVT) field varied between 13% in July and 17% in April for weather conditions in Spain. The highest thermal exergy production occurred in May due to cooler ambient temperatures compared to the highest solar fuel months from June to August. Martínez-Gracia et al. [24] proposed a hybrid PV/T solar field combined with a seasonal storage tank and a water-to-water heat pump. Simulation results demonstrated that this setup could meet 80% of the building's hot water demand. Menberg et al. [25] conducted a detailed exergy analysis of a hybrid system with a supplementary boiler operating in both heating and cooling modes. Their study reveals significant differences in the components that contribute the most to the overall exergy consumption in each mode. The comparison of exergy consumption shows that the distribution of exergy losses varies between heating and cooling operations, with distinct components contributing to the overall exergy inefficiencies in each mode. Lee et al. [26] investigated a hybrid system combining a hydrothermal heat pump and a pellet boiler, and their findings indicated that this system can be effectively applied to smart farm heating. The study demonstrated that the hybrid system not only performs efficiently in terms of heating but also offers significant energy cost savings, making it a viable solution for smart farm applications. Moreover, various types of heat pump–biomass hybrid systems are already available on the European market [27,28], showing great potential to accelerate the decarbonization of the building sector. These systems offer an efficient and sustainable way to reduce reliance on fossil fuels, thereby improving the overall energy efficiency of residential and commercial buildings.

From the state-of-the-art study conducted, it can be observed that hybridization with a biomass boiler is rarely considered, highlighting a significant research gap. Additionally, there is a lack of studies analyzing the configuration of hybrid systems—whether in series or parallel integration—while also accounting for the necessary auxiliary bypass systems when

the heat pump is stopped for technical reasons, from energy, economic, and environmental perspectives. Furthermore, optimization of the operating point based on the heat pump cut-off temperature, across all configurations, is also absent in the current literature. Therefore, this article presents a guide for selecting the most appropriate configuration based on the criteria adopted for such selection. A dynamic model of the seasonal energy performance of a HHP system composed by an air-to-water heat pump coupled to a backup device (a biomass boiler) is presented. Different configurations of the HHP have been developed to account for some key performance indicators (KPI), including efficiency, CO_2 emissions, operational costs, and more. The dynamic model of the hybrid system has been developed by means of TRNSYS 18 [29]. The main goal of this investigation is to analyze the role played by the backup biomass boiler, the system control logic, and the heat pump defrosting cycle with respect to the building's design heating load on the seasonal performance factor of the HHP system.

2. Methodology

2.1. Layout of Simulated Systems

Various configurations of heating systems, using air-to-water heat pumps, biomass boilers, and integrating both systems, were modeled to assess and contrast their impact on energy, environmental, and economic performance. Figure 1 illustrates the layout of the simulated systems. All components depicted in Figure 1 were provided within the TRNSYS libraries and custom dynamic models developed by the authors, as detailed in [30].

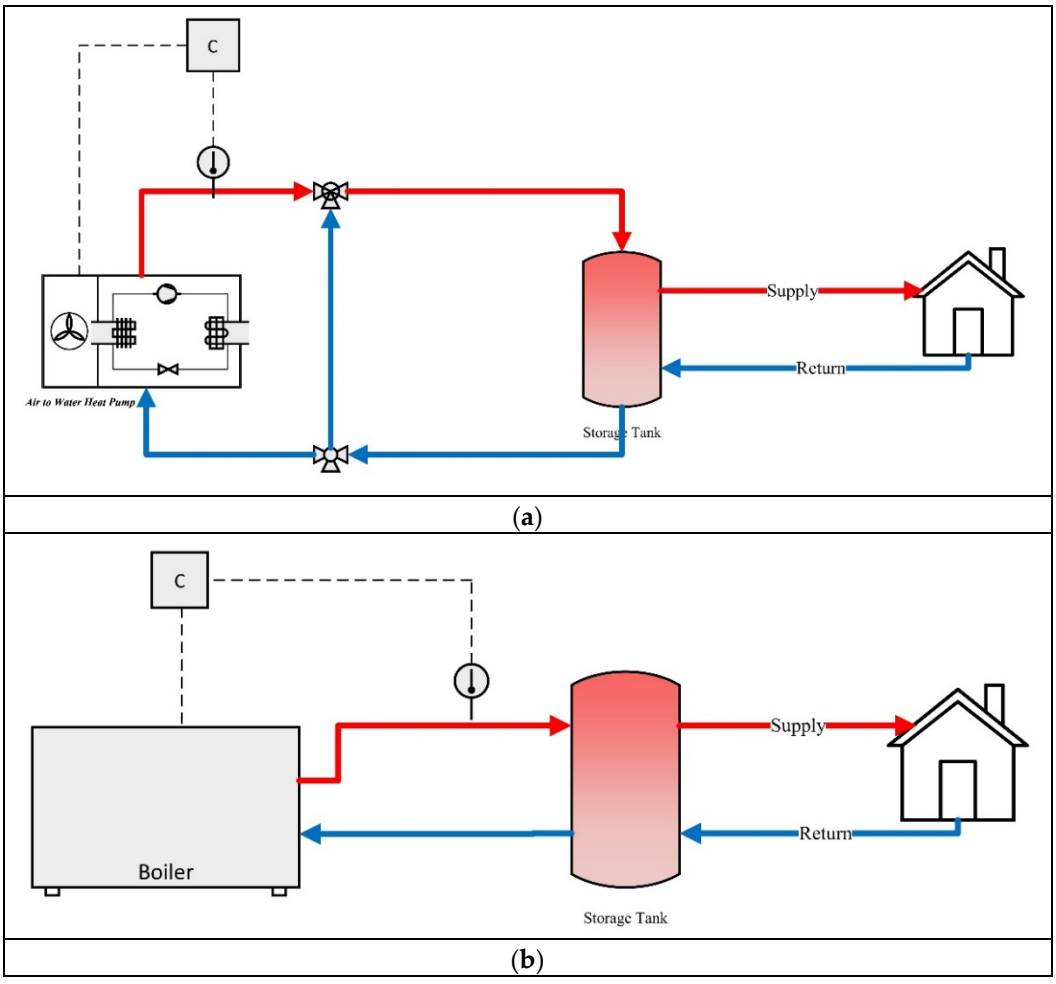

Figure 1. *Cont.*

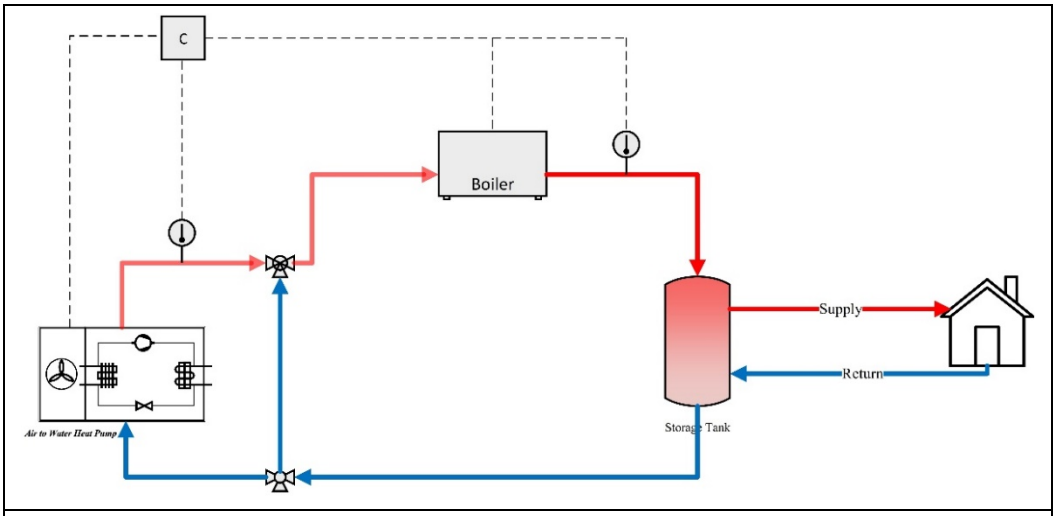

(**c**)

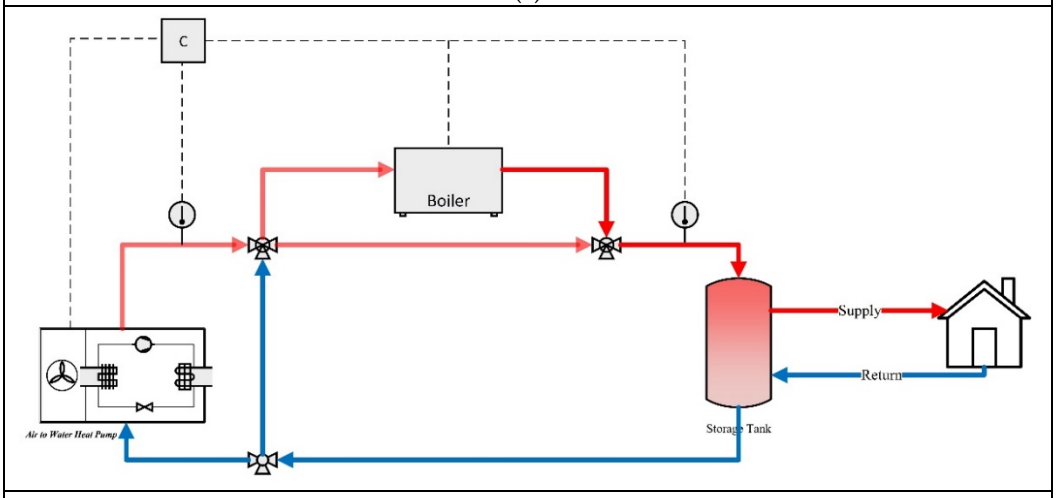

(**d**)

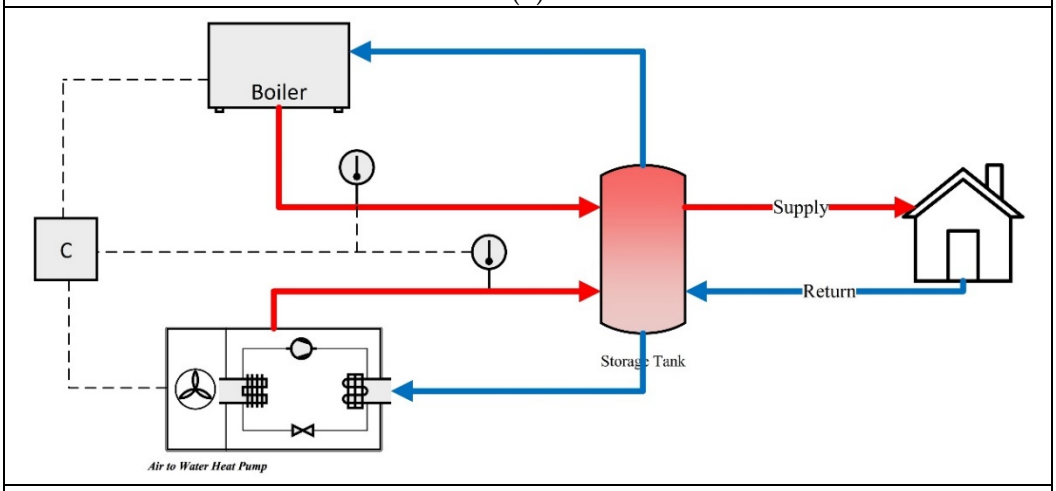

(**e**)

Figure 1. *Cont.*

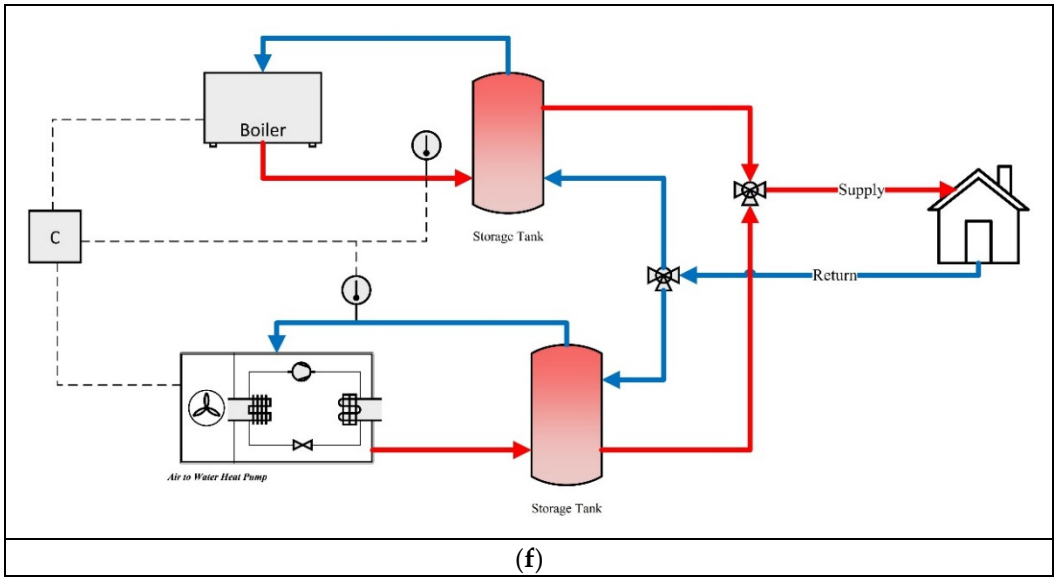

Figure 1. Layouts of the simulated heating systems: (**a**) configuration 0-HP, (**b**) configuration 0-Boiler, (**c**) configuration 1, (**d**) configuration 2, (**e**) configuration 3, (**f**) configuration 4.

Figure 1a depicts the monovalent systems, which serve as baselines for the energy performance analysis conducted in this paper. In these configurations, the heating system relies solely on a single heat generator, namely an air-to-water heat pump. In this scenario, the generator is sized to meet the building's heating peak load. Consequently, the energy demand of the building is fulfilled throughout the entire winter season. Another option is using a biomass boiler for the heating system in winter, which is illustrated in Figure 1b. In this configuration, a heat pump is used just for the cooling demand.

To consider the hybrid system concept, which involves the parallel or series operation of heat generators, four configurations were introduced. These configurations involve coupling an air-to-water heat pump with a backup device, specifically a biomass boiler. In these cases, the heat pump size is reduced because a portion of the heating load is covered by the backup system. In configurations 1 and 2, the heat generators are linked in series to enhance the energy performance of the heat pump by utilizing a lower sink temperature. Two bypass valves are employed: a cut-off bypass valve ensures that in cut-off situations, the flow rate of the heat pump is reduced to zero. Additionally, the boiler cut-off bypass valve (configuration 2) splits the water flow between the heat pump and the boiler based on the opening of the tempering valve. In this valve, the flow rate to the boiler is regulated according to the difference between the set point and the output temperature of the heat pump, ensuring that the temperature of the tank inlet remains at 55 °C. Configurations 3 and 4, on the other hand, are defined as independent systems, where each system has its own separate hot water cycle. In both configurations, the mass flow rates on the supply side (boiler and heat pump) are constant, and the outlet temperature of the heat pump is monitored to control the heat pump and boiler. If the temperature falls below the set point, the boiler is activated to support the heat pump, raising the outlet temperature. Once the outlet temperature reaches a nominal difference of 5 °C, the controller sends a stop signal to turn off the boiler. Configuration 4 uses two valves to mix the flow rate of the two sides (boiler and heat pump). A tempering valve is used to ensure that the supply temperature to the home is always maintained at 55 °C. Depending on the difference between the outlet temperature of the heat pump's tank and the set point, the tempering valve regulates the flow rate through the boiler tank. Additionally, the water flow rate serving the heating demand has been determined by maintaining a nominal temperature difference of 5 °C.

The heat pump utilized in the simulations is an inverter-driven unit based on a compression cycle. Its model employs a performance-map approach, detailed in [29]. The

heating capacity and Coefficient of Performance (COP) of the heat pump are determined using a three-dimensional lookup table. This table is a function of the inverter frequency (Φ), as well as the sink and source temperatures (i.e., supply water temperature, T_{wo}, and external air temperature, T_{ext}). These performance data were obtained from a heat pump manufacturer.

As the air-to-water heat pump is sized based on the building's design load, it adjusts its delivered thermal capacity during milder seasons to match the building's energy demand. Consequently, the heat pump undergoes numerous on–off cycles, particularly when further modulation of the compressor speed is not feasible. The energy performance of the unit diminishes with each startup due to the necessity of restoring the pressure difference between the high- and low-pressure sides. This degradation effect primarily results in a reduction in the unit's heating capacity, rather than an increase in the electrical power input [31].

Regarding the defrosting required for the HP in humid and cold periods, the reverse cycle method is the most commonly employed strategy for air-source heat pumps [32]. A simplified model based on this technique has been utilized in this study. This model accounts for frost formation and the associated energy losses during defrosting. During the defrosting process, the roles of the condenser and evaporator are reversed: the indoor heat exchanger acts as an evaporator, while the outdoor heat exchanger operates as a condenser. The heat pump is deactivated for one minute before the cycle inversion. Following this standby period (five minutes), the unit operates in cooling mode to melt the frost layer. Subsequently, after another standby period (one minute), the heat pump resumes operation in heating mode. Defrost cycles are executed by the heat pump at predetermined intervals (one hour), specifically when the outdoor air temperature falls below 5 °C and the relative humidity exceeds 75% simultaneously, but they can be modified accordingly.

2.2. Building Modeling and Climatic Data

The heating and cooling demands have been calculated by specific software (Design Builder (v.3.2)). Three different energy efficiency standards were studied to compute the heating and cooling demands of a two-story rural dwelling with a total useful surface of 150 m^2. However, only the worst standard corresponding to a building constructed before 1979 was used in this study. The U-values for the rural dwelling considered were based on the 1979 Spanish building standard (External walls 1.2, Roof 0.7, Ground floor 0.86, and Internal partitions 1.2 $W/m^2 \cdot K$). The infiltration rate is assumed to be 5.64 air changes per hour (ac/h) at 50 Pa, with a ventilation rate of 0.4 ac/h. The air permeability of windows and doors is set at 100 $m^3/h \cdot m^2$ [33]. The window-to-wall ratio is 15% for all the walls, and aluminum window frames (without a thermal break) with a U-value of 5.8 $W/m^2 \cdot K$ are used. The usage profile considered is included in the Spanish regulation [34] and consists of the following aspects:

- Heating is available from January to May and from October to December, with a set point of 20 °C from 8:00 a.m. to 11:59 p.m. and 17 °C from 0:00 a.m. to 7:59 a.m.
- Cooling is available from June to September, with a set point of 25 °C from 4:00 p.m. to 11:59 p.m. and 27 °C from 0:00 a.m. to 7:59 a.m. From 8:00 a.m. to 3:59 p.m., cooling is not available.
- A metabolic rate of 117.21 W/person and an occupancy density of 0.03 people/m^2 resulted in a thermal load per person of 3.51 W/m^2.
- A 100% occupancy is considered 24 h a day on Saturdays and holidays. A total of 61% of the occupancy load is sensitive, while 39% corresponds to latent load.
- Internal heat gains from equipment and lighting are 4.40 W/m^2. On the other hand, the lighting load is 50% transmitted by convection, 30% by long-wave radiation, and 20% by short-wave radiation.

The annual demands of this building for heating and cooling are 22,645 kWh and 1044 kWh, with peak demands of 12.35 kW and 5 kW, respectively. The indoor temperature was set to 20 °C from 8 to 22 h and 17 °C at night, which means that the daily heating

peak is found at 8 h when there are lower external temperatures and the indoor set-point temperature is raised 3 °C. Demands have been calculated for the Spanish climate of Teruel city (36,000 inhabitants). The Köppen climate classification for the Teruel capital is Cfb (oceanic climate) with continental influences, thereby considering milder summers with winters in acclimatization. Hourly demands during the year were then linked with TRNSYS, as well as the local temperature and humidity ratio in the zone to control the part load operation and defrosting activations of the HP. A schematic of the modeled building is given in Figure 2.

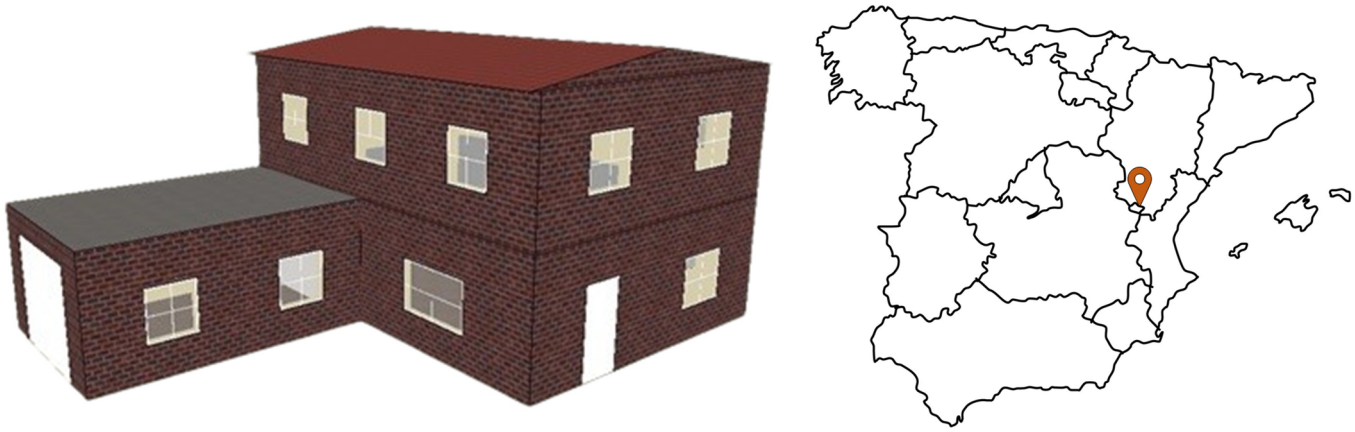

Figure 2. Two-story rural dwelling.

2.3. Heating System Configurations

In order to study the influence of the heat pump size on the seasonal energy performance of an HHP system, four air-to-water heat pumps (HP) from a HP manufacturer have been considered in this work, coupled to a biomass boiler (B). The main characteristics of the simulated units are summarized in Table 1, with the coefficient β being the ratio between the heat pump's heating capacity at design conditions and the building's peak load. In Figure 3, the heating capacity at the full load of the heat pumps is reported as a function of the ambient temperature. It is clear that by increasing the heat pump capacity from 4 to 12 kW, the value of T_{biv} strongly increases, and, for this reason, the peak load ratio (β) decreases. The bivalent temperature of the system for all hybrid heat pump systems is listed in Table 1; for higher HP capacities, it is reduced. The bivalent temperature (T_{biv}) is the point where the building's heating load (solid line) intersects with the heat pump's heating capacity (dashed line). The cut-off temperature ($T_{cut-off}$) is the ambient temperature at which the heat pump is deactivated according to energy or economic considerations. The cut-off temperature for monovalent systems is −5 °C and for hybrid systems is $T_{cut-off} = 0$. When the outdoor air temperature falls below the cut-off temperature, the backup device becomes the sole active heat generator. The hybrid system operates by activating the backup heater and heat pump when $T_{cut-off} < T_{ext} < T_{biv}$. When the outdoor air temperature (T_{ext}) is lower than the cut-off temperature, the biomass boiler is the only heating system in operation, and the heat pump is shut down. For $T_{ext} > T_{biv}$, the heat pump is the sole heating source while the biomass boiler remains off. The temperature of the hot water supplied by the heat pump is continuously monitored and compared with a predetermined set-point value. If the heat pump cannot meet this set point (indicating its heating capacity is insufficient), the backup boiler is activated.

In the single configuration, both the heat pump and biomass boiler were sized to meet the building demand entirely. However, in the hybrid configuration, undersized heat pumps were deliberately chosen. The backup biomass boiler was then utilized to fulfill the remaining portion of the demand, ensuring the complete satisfaction of the building's energy requirements.

Table 1. Technical data of the selected air-to-water heat pump and biomass boiler systems.

Heat Generators	P_{HP} (kW)	P_B (kW)	β	T_{biv}
Heat pump	12	13	1	−2
Boiler	0	13	0	-
Heat Pump + Boiler	4	13	0.33	9.3
Heat Pump + Boiler	6	13	0.5	7.4
Heat Pump + Boiler	8	13	0.66	4.9

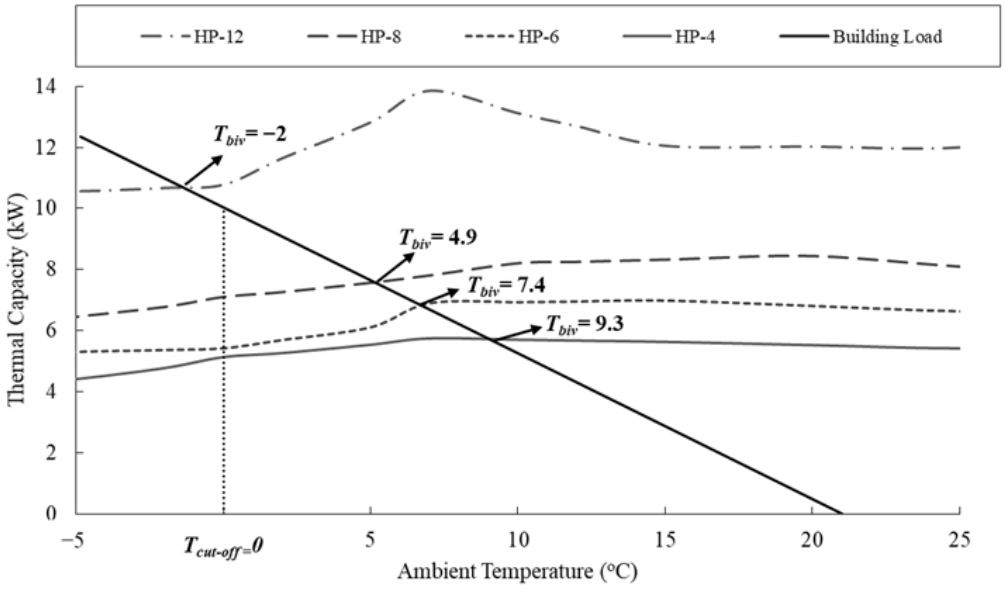

Figure 3. Performance data at full load of the considered heat pumps and building energy signature (BES).

2.4. Control Strategies of the Heating Systems

The heat pump control strategy utilizes a *PID* controller combined with an on–off algorithm. Figure 4 illustrates the flow chart representing this control logic. The control system of the heat pump utilizes the supply water temperature at the outlet of the unit ($T_{wo.HP}$) as the monitored variable, comparing it to the set-point value imposed. The *PID* algorithm adjusts the inverter frequency to regulate the heat pump's heating capacity based on the building's heat load. During periods of low energy demand and when the minimum frequency is achieved, the heat pump operates at a fixed speed, and the on–off control logic becomes active. This on–off algorithm includes a hysteresis cycle with a 5 K amplitude, centered on the supply water's set-point temperature.

In hybrid configurations, the two devices function autonomously and need separate activation. The boiler employs on–off cycles to manage the building's heat load. The type 122 boiler was chosen, operating at a constant efficiency of 92% and capable of operating at a minimum part load of 20%. The monitored variable during this mode of operation is the water temperature outlet from the heat pump, T_{wo}. The boiler is turned off when T_{wo} exceeds $T_{w,set}$, and it is subsequently turned on when T_{wo} is lower than $T_{w,set} - 5$ K. Additionally, the backup device is only activated when the heat pump is running and its heating capacity is insufficient to meet the building's load. Moreover, a cut-off temperature ($T_{cut-off}$) is incorporated into the system. When the outdoor temperature drops below $T_{cut-off}$, the heat pump is completely disabled (an excessive number of defrosting cycles will be avoided).

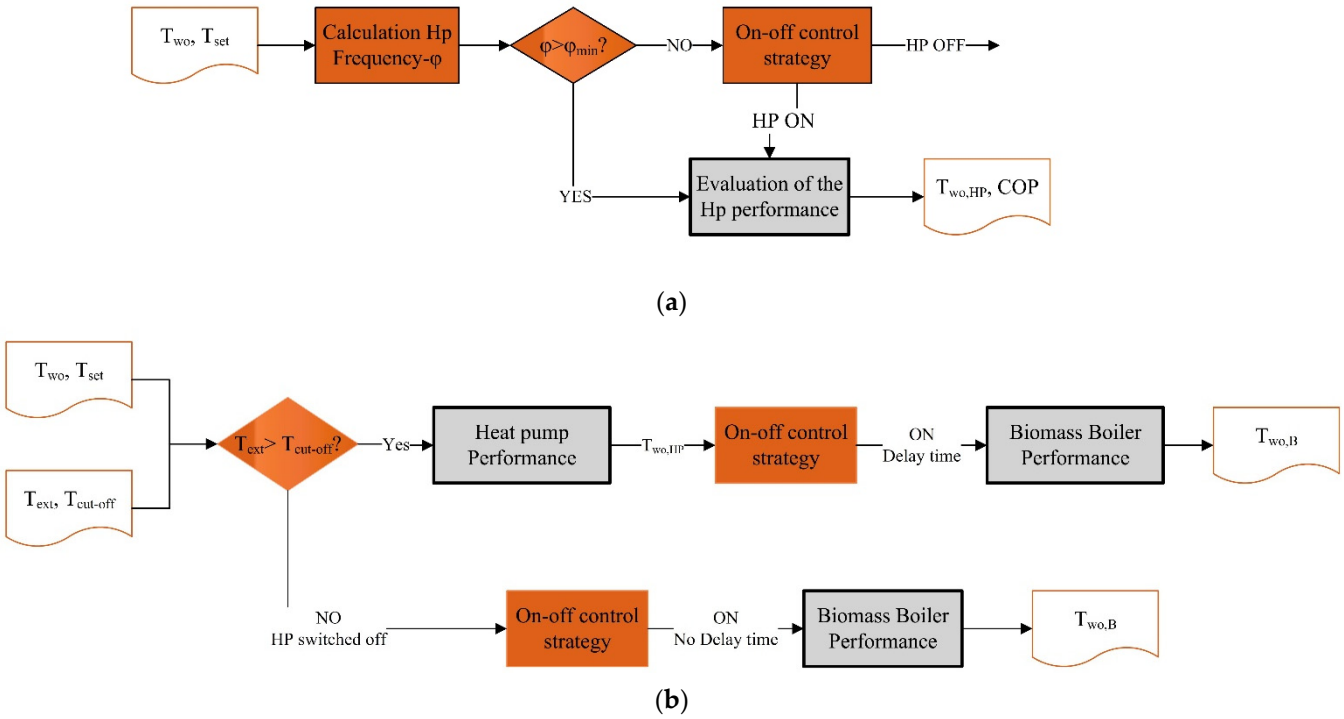

Figure 4. Control algorithm implemented in TRNSYS for the AWHP (**a**) and the hybrid system configurations (**b**).

The fundamental elements of the heating systems were represented using standard components: Type 158 for the buffer tank (150 L), while system control logics were implemented through Type 2 (hysteresis thermostat) and Type 23 (PID controller). A stratified storage tank was used (10 nodes; TRNSYS model Type 158) with 2 inlets, 2 outlets, and an assumed overall tank heat loss coefficient of between 2.5 and 3 kJ/h.m^2. K. The performance of the biomass boiler was assessed using the boiler block (Type 122). For the evaluation of the heat pump's cooling capacity and Energy Efficiency Ratio (EER) under various operating conditions, Type 581 (Multi-Dimensional Data Interpolation) was employed. This type facilitates multi-dimensional linear interpolation between the user-supplied performance data across several values of independent variables (e.g., T_{ext}, T_w, and Φ). Additionally, the authors have modified the code to simulate defrosting behavior.

2.5. Key Performance Indicators

To assess the seasonal efficiency and energy performance of hybrid configurations during a year, where the various heaters (biomass boilers and heat pumps) are powered by different energy sources (electric energy (EE) and biomass), the EU standards on energy efficiency for heating and cooling systems were first calculated. The system's seasonal efficiency for heating (η_s) is defined in Equation (1) as the ratio between the total thermal energy supplied by the heating system to the building ($E_{th,tot}$) and the total primary energy consumption of the system ($E_{p,tot}$):

$$\eta_s = \frac{E_{th,tot}}{E_{p,tot}} \quad (1)$$

To account for $E_{p,tot}$, the Primary Energy Factors (PEF_{el}, PEF_b) for electricity and biomass for Spain have been taken [35]. Additional HP performance indicators can be

associated for HHP systems. The $SCOP_{net}$ is the net seasonal coefficient of performance of the HP operating in monovalent mode:

$$SCOP_{net} = \frac{E_{th,HP}}{E_{HP,ee}} \quad (2)$$

According to European standard EN 14825 [36], the adequate assessment of the efficiency in hybrid systems is the $SCOP_{on}$ for hybrid heating systems, which is closely related to η_s and can be calculated as follows:

$$SCOP_{on} = \frac{\sum_{j=1}^{n} h_j \times E_{th,tot}(T_j)}{\sum_{j=1}^{n} h_j \times \left[\frac{E_{th,HP}(T_j) - E_{th,\,B}(T_j)}{COP_{HP}(T_j)} + \frac{E_{th,\,B}(T_j)}{\eta_B \times CC}\right]} \quad (3)$$

where h_j is every hourly period simulated in TRNSYS at temperature T_j; $E_{th,B}$ is the heating supplied at temperature T_j by the boiler (kW); COP_{HP} is the COP of the HP at every T_j; η_B is the seasonal heating efficiency of the boiler in active mode, in %; and CC is the conversion coefficient from primary to final energy, equal to 2.5 for EU.

The Seasonal Energy Efficiency Ratio (SEER) for cooling is calculated by the following:

$$SEER = \frac{E_{HP,C}}{E_{HP,C,ee}} \quad (4)$$

where $E_{HP,C,ee}$ and $E_{HP,C}$ are the electric energy consumptions of the heat pump and the energy delivered by the heat pump, respectively.

The Annual Performance Factor (APF), which describes the annual energy performance of the system by considering both heating and cooling behavior, is defined as follows:

$$APF = \frac{E_{th,HP} + E_{HP,C} + E_{th,\,B}}{E_{HP,th.ee} + E_{HP,c,ee} + E_{B,input}} \quad (5)$$

where $E_{HP,th.ee}$ and $E_{HP,c,ee}$ are the annual electricity consumptions for heating and cooling; and $E_{B,input}$ is the required boiler energy input. This accounts for the conversion from secondary to final energy, which is somewhat analogous to $SCOP_{on}$. However, we do not apply a conversion factor for primary energy in the biomass boiler equivalent to electricity, and we also consider the cooling period. When the boiler is used extensively, the Annual Performance Factor (APF) is lower than $SCOP_{on}$ because its usage is penalized [11].

Regarding the CO_2 emissions, we used as environmental KPI the Equivalent Warming Impact on the System (EWI), which evaluates the environmental impact of the various fuels used in the system throughout its life cycle [37]. For each fuel, the GWP or equivalent quantity of carbon dioxide per quantity of final energy ($kgCO_2/kWh_{FE}$) for a time frame of 100 years, coming from the Ecoinvent Data Base (2013) [38], widely used in LCA, was taken. Thus, the EWI is the ratio of greenhouse gas emissions to the useful energy output of the system:

$$EWI = \frac{(E_{HP,th.ee} + E_{HP,c,ee}) \times GWP_e + E_{th,B} \times GWP_b}{E_{tot,th} + E_{toc,c}} \quad (6)$$

where $GWP_e = 0.521$ and $GWP_b = 0.041$ $kgCO_2/kWh_{FE}$ [38]. As an example, GWP_e is the global Warming Potential for electricity, and represents the weighted addition of the emission of different greenhouse gases when providing the final energy, including emissions generated during the construction of the electric grid and power plants.

Finally, the simple estimation of the operating costs of the solution adopted takes into account the local prices of electricity and biomass (p_{ee}, p_b):

$$OC = (E_{HP,th.ee} + E_{HP,c,ee}) \times p_{ee} + E_{th,B} \times p_b \quad (7)$$

where $p_b = 0.07$ €/kWh, the average commercial price for biomass pellets in Spain in 2023; and p_{ee} is the hourly electrical price for Spain in 2023 [39].

3. Results and Discussion

A series of simulations was conducted to examine how the backup typology and heat pump size affect the seasonal energy efficiency of the entire system. In all scenarios, the cut-off temperature for the HHP systems was set to the outdoor design temperature. In hybrid setups, both heaters operated simultaneously throughout the heating season, with the heat pump given priority as the primary heating source.

Figure 5 presents a comparative analysis of the thermal energy production for the various hybrid heat pump–boiler configurations. It illustrates the energy contribution from heat pumps and boilers across different system designs and heat pump capacities. It is seen that all configurations can cover the heating demand of the building for the whole year. In the hybrid configurations, the heat pumps are sized to cover only a portion of the design load (33%, 50%, and 66%) and a biomass boiler is used as a backup to meet the remaining heating demand. This co-working results in better efficiency for the hybrid system, as highlighted in previous research [6,11]. Moreover, in all configurations, as the heat pump capacity increases from 4 kW to 8 kW, the heat pump's contribution generally increases while the boiler's decreases.

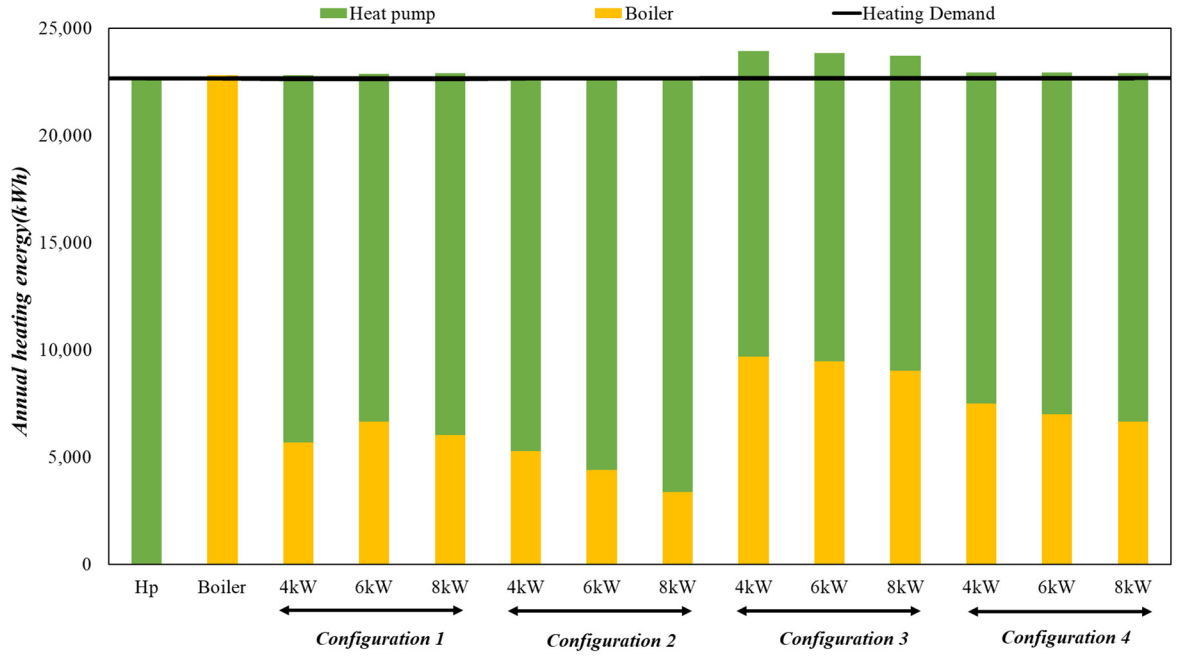

Figure 5. Thermal energy production delivered to the building for various hybrid heat pump–boiler configurations.

3.1. Configuration Analysis

Figure 6 illustrates the seasonal energy efficiency of the system (η_S) and the total number of on–off cycles performed by the heat pump and the biomass boiler as functions of the building peak load ratio (β) across all configurations. Figure 6a shows that as β increases, the η_S values for all configurations generally rise, albeit not uniformly [7]. Configurations 1 and 2 exhibit very similar trends, peaking at $\beta = 0.33$ and $\beta = 0.66$, with slight dips at $\beta = 0.5$. Configuration 3 has the lowest η_S values for most of the range, while configuration 4 follows a pattern between configurations 1 and 3, with less pronounced peaks and valleys. Overall, the η_S value for the serial configurations (1 and 2) is better than for the parallel configurations (3 and 4). Notably, the best performance is achieved with a 8 kW heat pump in the serial system, whereas in the parallel system, the 4 kW heat pump performs better.

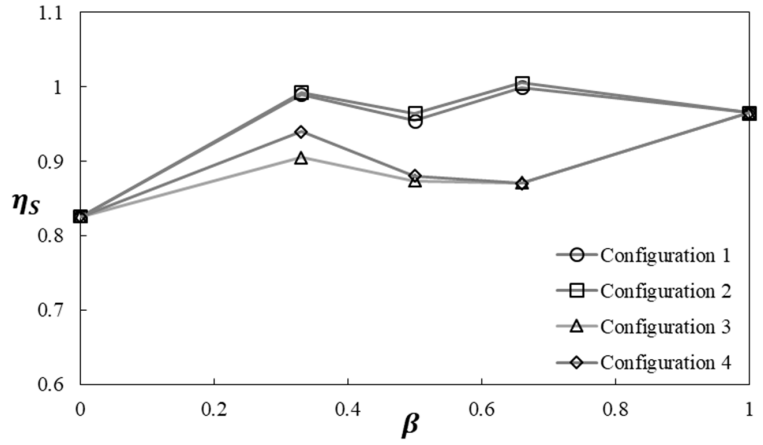

(**a**)

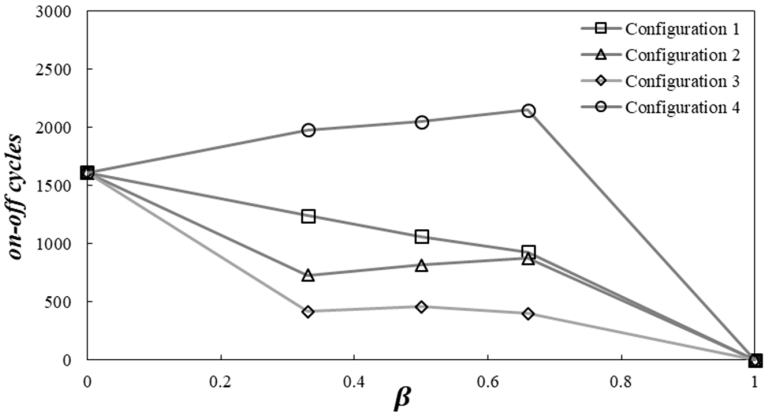

(**b**)

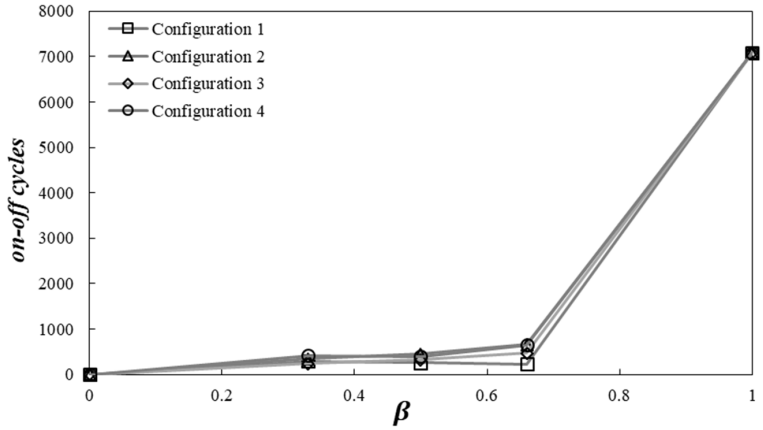

(**c**)

Figure 6. Comparison of HHP characteristics for different configurations as functions of the building peak load ratio: (**a**) seasonal energy efficiency of the system, (**b**) boiler on–off cycles, and (**c**) heat pump on–off cycles.

The frequency of biomass boiler cycling is shown in Figure 6b. For configuration 4, the on–off cycles of the boiler increase as the heat pump capacity rises, while the other configurations exhibit a decreasing pattern. Although the highest values occur for the monovalent system (with only a boiler) compared to configurations 1, 2, and 3, configuration 4 reaches its peak at $\beta = 0.66$. Figure 6c likely depicts the frequency of heat pump cycling (on–off operations) for various value of β. As β increases, the on–off cycles generally rise across all configurations. A dramatic increase is observed for the monovalent system, where the 12 kW heat pump

cycles on and off much more frequently to meet the demand. Additionally, configuration 1 exhibits the lowest on–off cycles for most of the range, especially diverging from the other configurations at $\beta = 0.66$. Moreover, the hybrid configuration reduces the number of on–off cycles performed by the heat pump. This reduction is due to the smaller size of the heat pump relative to the design heat load. Indeed, with undersized heat pumps, on–off cycling must be used to adapt the unit's heating capacity to the building's heat load only during the milder part of the heating season. When undersized devices are used in HHP systems, the energy losses associated with on–off cycles are reduced, thereby improving the energy performance of the heat pump. It is worth mentioning that the number of defrost cycles performed by the heat pump does not change, as the control strategy for activating the defrosting process depends on outdoor conditions and the HP operation. The parameters of this algorithm remain consistent for each case.

The ratio of the greenhouse gas emissions to the useful energy output of the system (EWI) and the operation cost of heating and cooling of the building are indicated in Figure 7.

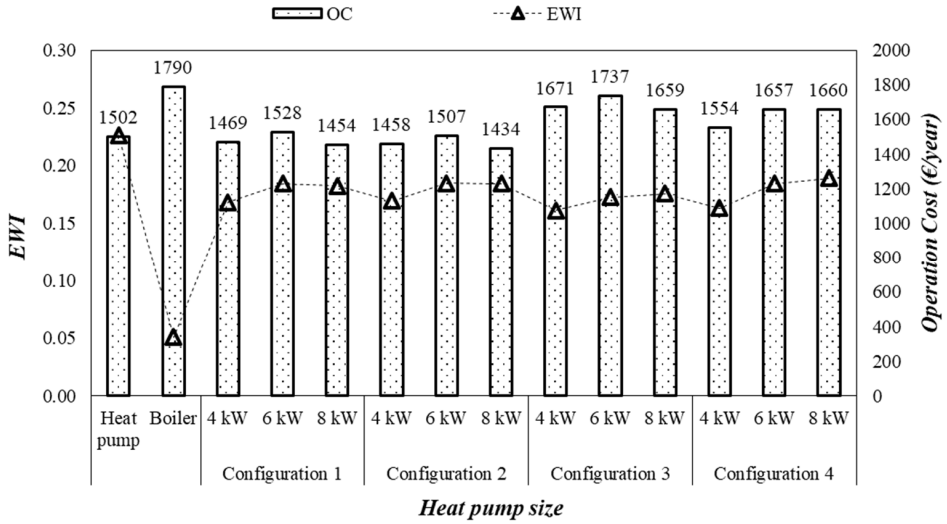

Figure 7. The Equivalent Warming Impact on the System and the operation cost of different configurations (EUR/year).

The EWI considers the greenhouse gas emissions caused by the resource consumption of the different configurations when meeting the building's demand. As we expected, the lowest CO_2 emission was related to using the biomass boiler as a heating system (EWI = 0.05) and the emissions increased more than four times when monovalent heating systems based on the heat pump were used. Generally, the EWI increases when the heat pump's power rises from 4 kW to 8 kW due to the reduced contribution of the biomass boiler to heating. Furthermore, the EWI remains almost constant across all configurations, with no meaningful differences observed. According to the operational cost data, the operational cost of the HHP system is always lower than that of the monovalent system when a boiler is used as the heating system. Additionally, the operational cost in serial operations (configurations 1 and 2) is lower than in parallel operations (configurations 3 and 4) due to the heat pump's higher share in heat production (Figure 5). An interesting point in Figure 7 is that, for the HHP system, series operation is more efficient than parallel operation because it results in lower costs and reduced emissions. The main reason for this is the faster ability of the system to reach the $T_{wo,sp}$ before the buffer tank, which cannot be reached in the case of parallel configurations. This also forces the biomass boiler to work for more time periods since its activation occurs with more frequency, as we see in Figure 5.

In a nutshell, and based on the results in this section, we conclude that configuration 2 is the best option for the HHP system, as it offers the highest efficiency, lowest emissions, and the most reduced costs compared to the other configurations.

3.2. Effect of Cut-Off Temperature

The effect of cut-off temperature on the seasonal energy performance of HHP systems is more important than in monovalent systems since it directly affects the participation of the backup system. Based on weather conditions, two additional cut-off temperatures apart from 0 °C ($T_{cut-off} = \pm 3$ °C) were introduced, and their results were compared to the baseline simulation. The influence of $T_{cut-off}$ and the heat pump capacity on the seasonal energy performance and the on–off cycles of the HHP system is illustrated in Figure 8. According to Figure 8a, the general trend shows that in almost all configurations, the η_S improves by decreasing the $T_{cut-off}$, with the highest value of the heating seasonal efficiency belonging to configuration 2. In fact, for each heat pump capacity representing the bivalent temperature, η_S increases as $T_{cut-off}$ decreases, with the maximum value occurring at $T_{cut-off} = -3$ °C. The energy performance results can be fully explained by observing Figure 8b, in which the values of $SCOP_{net}$ are shown as functions of the heat pump capacity and the cut-off temperature. It is evident that for each heat pump size, the seasonal energy performance increases as the cut-off temperature increases [40]. There are two reasons for the improvement in $SCOP_{net}$ when the heat pump size is reduced. First, as $T_{cut-off}$ increases, the number of defrost cycles performed by the heat pump decreases. Second, because of low external temperatures and high compressor frequencies, the periods during which the heat pump operates with low COP values are significantly reduced. It is important to mention that when the cut-off temperature increases, the peak load ratio decreases, and the share of heating produced by the boiler increases, as shown in Figure 8c. For this reason, the energy performance of the whole HHP system is more influenced by the boiler's seasonal efficiency. Another interesting point is that the net seasonal coefficient of performance of the series operation (configurations 1 and 2) is much better than that of the parallel ones (configurations 3 and 4). In series operation, the HHP system with configuration 2 shows the best performance, and cut-off temperature changes have a greater impact on it. Also, the best $SCOP_{net}$ results are for the 8 kW heat pump, when $\beta = 0.66$. In parallel arrangements, $T_{cut-off}$ does not have a significant effect on $SCOP_{net}$. In contrast to the series configuration, the best performance was achieved at $\beta = 0.33$ with a 4 kW heat pump. Additionally, using two storage tanks and control valves to regulate the mass flow based on the building's demand improves the HHP's performance.

In Figure 9a, the yearly frequency of defrost and on–off cycles for air-to-water heat pumps is shown as a function of both the cut-off temperature and the heat pump's capacity. It is evident that as the cut-off temperature increases, the number of defrost cycles performed by the heat pump decreases. For example, the number of defrost cycles decreases by 21% when the cut-off temperature is increased from −3 °C to 0 °C, and by 73% when the cut-off temperature is increased to 3 °C. Moreover, the data shown in Figure 9a indicate that in configuration 2, the number of heat pump on–off cycles increases when the HHP system uses a larger heat pump. This trend is more pronounced at lower cut-off temperatures because the heat pump provides a larger portion of the heating demand and operates more frequently. For a constant heat pump capacity, there is a slight decrease in the number of on–off cycles performed by the heat pump during the heating season as the cut-off temperature rises [41]. According to Figure 3, increasing the cut-off temperature reduces the difference between the cut-off and bivalent temperatures, resulting in the heat pump having a smaller role in meeting the demand. There is no significant difference in the number of on–off cycles across the various configurations, as they are nearly identical; however, configuration 1 shows fewer on–off cycles than the others do. Looking at Figure 9b, the number of on–off cycles performed by the boiler decreases as the cut-off temperature increases. This means that at higher cut-off temperatures, the biomass boiler operates for more hours and has a larger share in meeting the building's demand. Additionally, in configuration 4, the biomass boiler cycles on and off more frequently than in the other configurations, with configuration 3 experiencing the fewest cycles, since the inertia of the buffer tank and the temperature drop to start up the boiler reduces its activation. Furthermore, in this case, the location of the inlets and outlets for

both the heat pump and the biomass boiler as well as the demand to use the buffer tank are key values that are not so crucial for the other configurations.

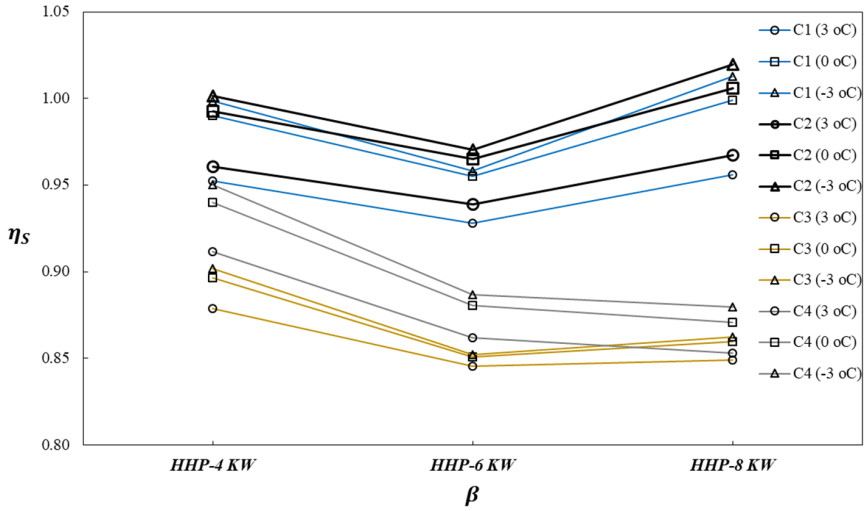

(**a**)

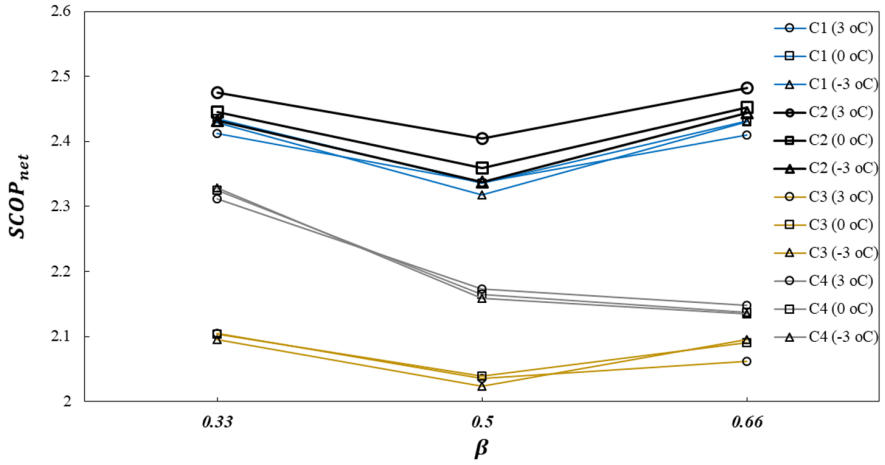

(**b**)

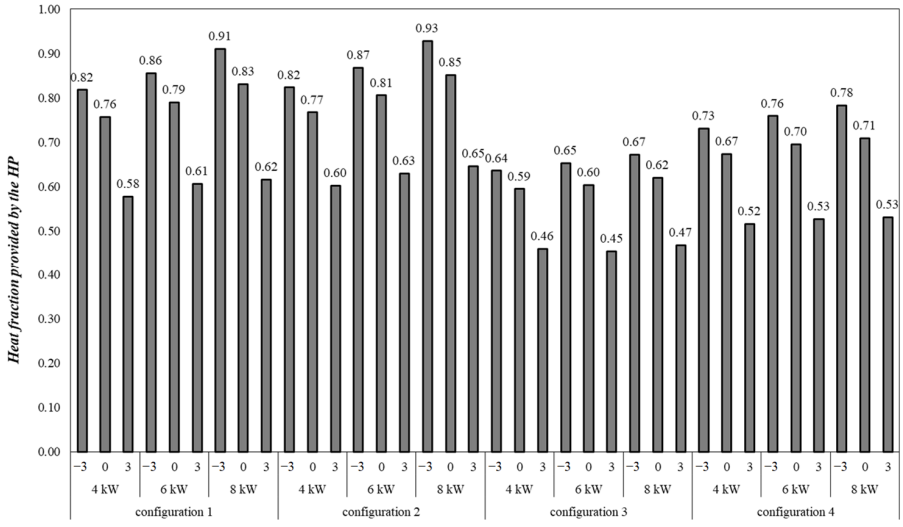

(**c**)

Figure 8. The effect of the cut-off temperature on the seasonal energy performance indicators: (**a**) η_S, (**b**) $SCOP_{net}$, (**c**) heat portion provided by the HP.

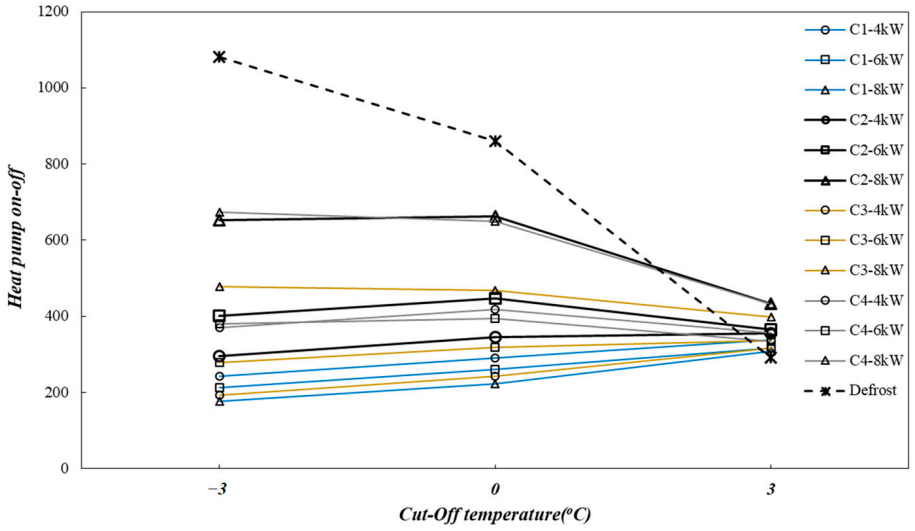

(**a**)

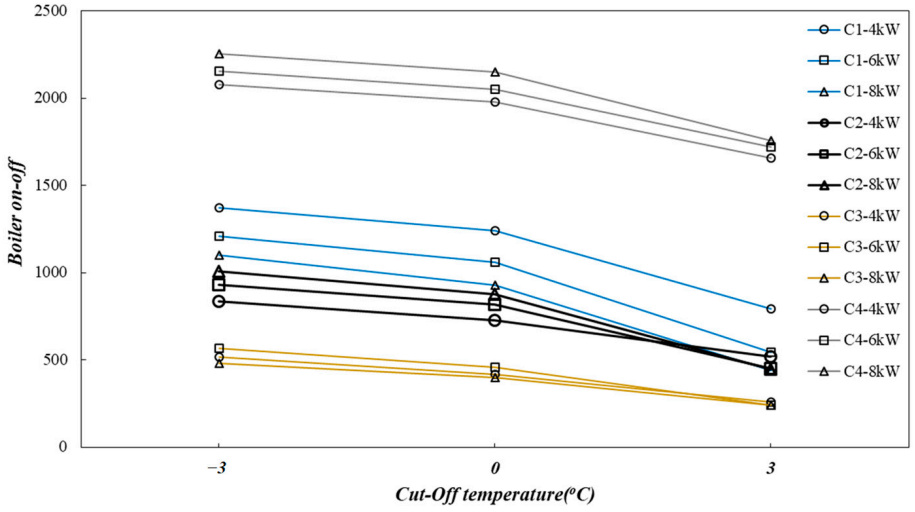

(**b**)

Figure 9. The effect of cut-off temperature and heat pump size on number of cycles: (**a**) heat pump on–off cycles, (**b**) biomass boiler on–off cycles.

For considering the effect of cut-off temperature on the environmental and economical KPIs, Figure 10 illustrates the EWI and OC as functions of both the heat pump size and the cut-off temperature. As expected, all configurations exhibit a decline in the Equivalent Warming Impact as the cut-off temperature increases because the biomass boiler plays a larger role in the HHP system compared to the heat pump (Figure 10a). Moreover, the EWI improves with a smaller heat pump size because less electricity is consumed. The effect of cut-off temperature on the operational cost is depicted in Figure 10b. It can be seen that the operational cost increases with rising cut-off temperature due to increased biofuel consumption [42]. The most important point is that configuration 2 is the cheapest among all configurations, and the HHP system with an 8 kW heat pump has the lowest operational cost.

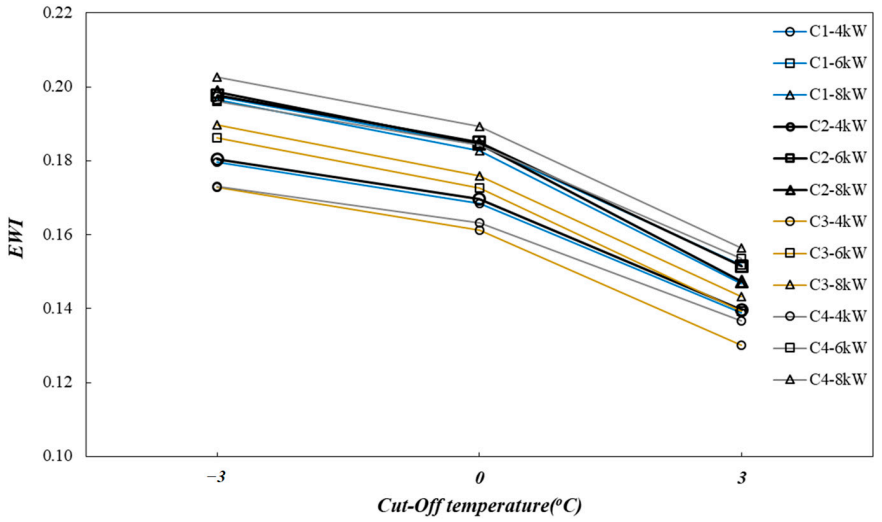

(**a**)

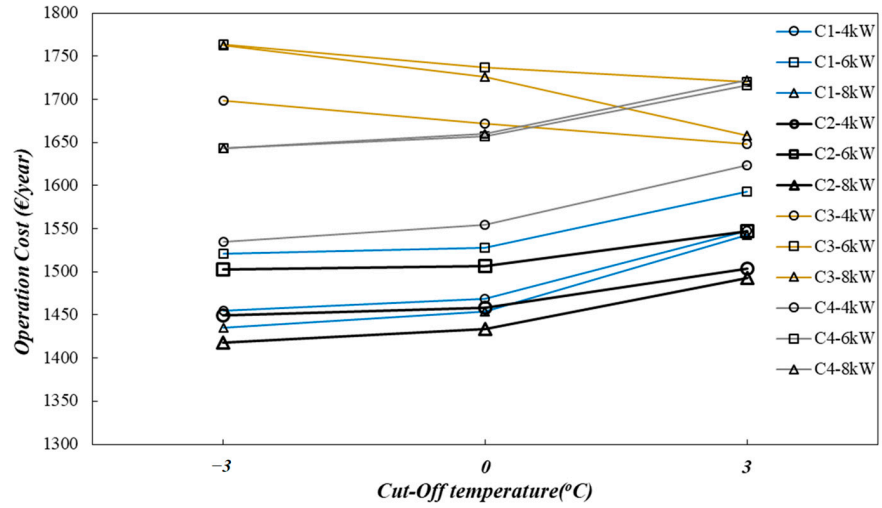

(**b**)

Figure 10. The effect of the cut-off temperature and heat pump size on the environmental and economical KPIs: (**a**) EWI, (**b**) OC.

3.3. Impact of Defrosting

To study the effect of defrosting on the HHP system, configuration 2 was analyzed for both heat pumps with and without a defrosting cycle. The results are presented in Figure 11. When the heat pump operates in reversible mode, defrosting is typically achieved by inverting the cycle. As seen in Figure 11a, defrosting negatively impacts HHP performance across all heat pump sizes, with a nearly 3% reduction in $SCOP_{net}$ at $T_{cut-off} = -3$ °C. For higher $T_{cut-off}$ values, the effect of defrosting is reduced. This outcome can be explained by two factors: a reduction in the energy supplied to the building and a decrease in heating demand due to the energy removed by the heat pump in cooling mode, since weather conditions do not force the system to activate defrosting [40]. Additionally, electrical consumption rises because of the energy required to melt or prevent the frost [43]. When the heat pump uses a defrost cycle, the number of on–off cycles for both the heat pump and the boiler increases with the size of the heat pump (Figure 11b). However, the opposite trend is observed for heat pumps that do not use a defrost cycle. This is due to the wider extension of humid and cold working periods for larger sized HP pumps. Looking at Figure 11c, it can be observed that the EWI remains unchanged for the heat pump, regardless of whether a defrost cycle is used. As expected, the operating cost

for a heat pump with a defrost cycle is higher due to the increased electrical consumption needed to melt the frost and the reduced overall efficiency.

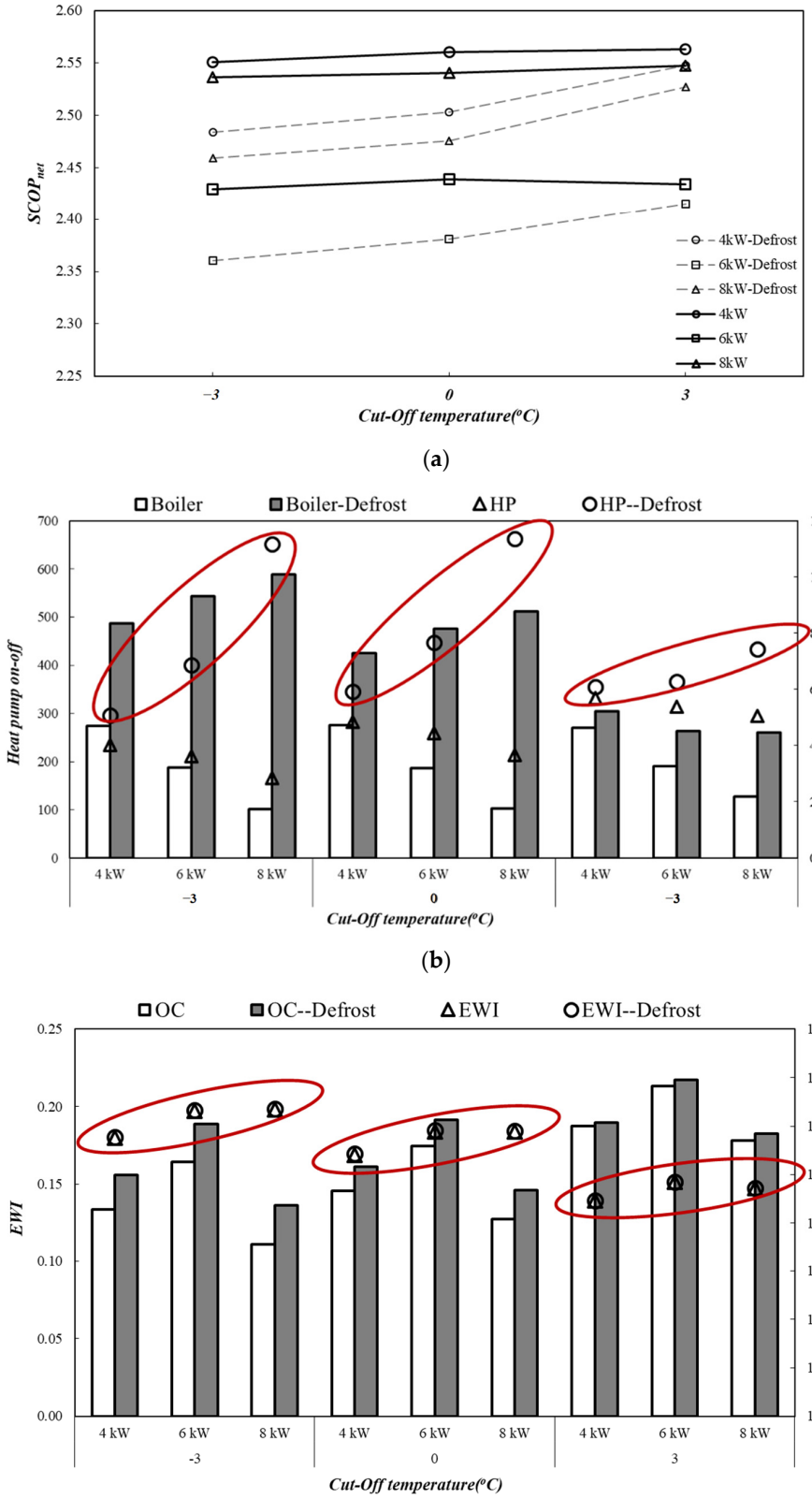

Figure 11. Considering the effect of defrosting cycles for configuration 2: (**a**) $SCOP_{net}$, (**b**) on–off cycles, (**c**) EWI & OC.

3.4. Heat Map

Figure 12 illustrates a heat map showing the key parameters used to evaluate the performance of configurations with respect to heat pump size and cut-off temperature. The heat map provides a visual comparison and detailed analysis of multiple parameters simultaneously. A green color gradient is used to indicate the best choices, where darker green represents better or more desirable values and lighter green represents less optimal values. The optimum condition for HHP systems occurs when η_S, $SCOP_{net}$, and APF (annual performance of HHP) are at high values and OC and EWI are at low values. Overall, the heat map reinforces that serial operation generally performs better across most metrics, especially at higher power levels and cut-off temperatures. Moreover, configuration 2 often outperforms configuration 1 in serial operation, and in parallel operation, configuration 4 generally shows better performance than configuration 3.

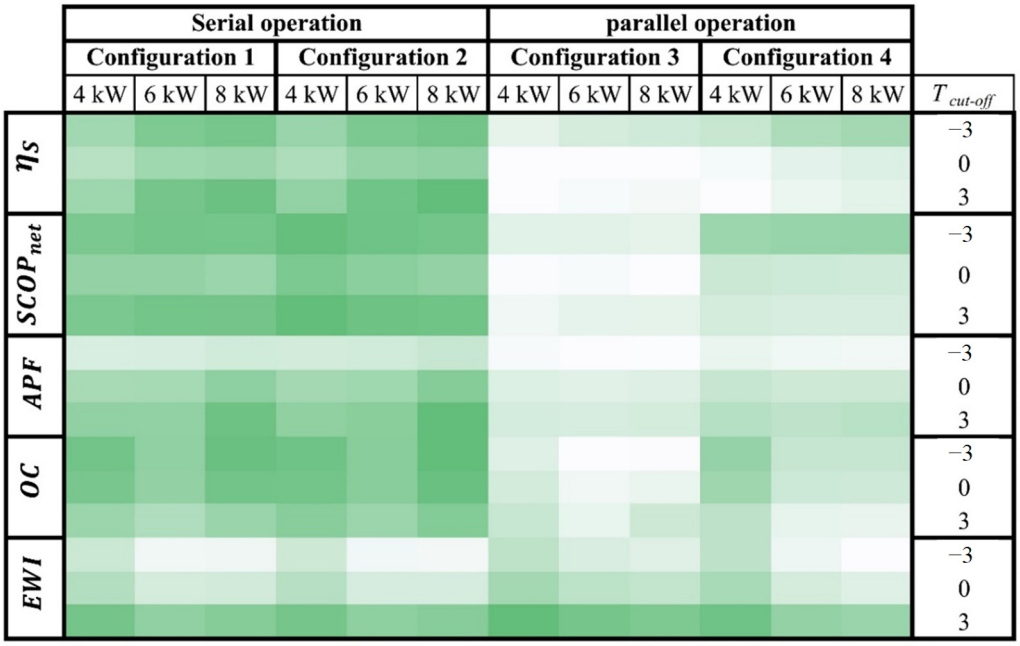

Figure 12. Heat map of HHP performance across the different configurations and conditions.

3.5. Limitations of the Study

While this research provides valuable outcomes about the configuration analysis of HHP systems, several limitations should be considered when interpreting the results. These limitations are the practical or theoretical shortcomings of the study that are often beyond the authors' control. Although these weaknesses may limit the generalizability of the conclusions, they also provide a foundation for future research. These limitations are as follows:

- While various configurations for HHP systems are examined, there may be other potential configurations not covered in this study. Some key design parameters like the tank volume or outlet temperatures for heating and cooling seasons could lead to alternative optimal design solutions.
- The results are very sensitive to the technical data of an AWHP commercial series, and may not be applicable to other HP manufacturers. For instance, the low performance values of the 6 kW heat pump (but with a large operational range) are responsible for some of the observed outcomes in this study (see Figure 5). Another handicap was found in not having an equilibrated operating window for the AWHP series from the manufacturer, in the sense that an AWHP could demonstrate operation at 30%, with $T_{wo} = 55\ ^{\circ}C$ and $T_{ext} = 3\ ^{\circ}C$, but some others could not. Therefore, the use

of the AWHP is limited in some cases and then the BB increases its operation, since interpolation is not feasible in the TRNSYS model.

- The study focuses on air-to-water heat pumps with constant efficiency biomass boilers as backup. We considered that radiators were maintained in the studied rural dwelling, served at 55 °C. Other types of heat pumps or backup systems might yield different results. Cooling performance was also studied but a similar pattern was found for any configuration since the hybrid configuration is not feasible. Nonetheless, a balanced heating and cooling demand is desired, as shown in the APF that accounts for both seasons.
- The economic analysis used specific energy prices, but obviously, these depend on market and geopolitical conditions and thereby vary over time and by location. A constant price for electricity was firstly used (average value for Spain in 2023), but no major differences were found with respect to the figures presented here. A PV supply for the HP could strongly reduce the OC of the system but the investment should be then included in the economic KPI.
- Although this research utilizes a PID controller combined with an on–off algorithm with specific dead bands, there may be more advanced or alternative (predictive) control strategies that could further optimize system performance. Nonetheless, here a simple control based on T_{wo} was used in order to compare the set of analyzed configurations as fairly as possible.

4. Conclusions

In this paper, a numerical study on the energy performance of hybrid heat pump systems has been conducted using a series of dynamic simulations with TRNSYS. The hybrid systems investigated are based on an air-to-water heat pump (AWHP), with a biomass boiler considered as a backup device. This type of hybrid installation is specifically designed for isolated homes, where it is highly likely that there is no connection to the grid and no access to the gas distribution networks. In such cases, electricity generation to power the efficient heat pump can be partially supported by photovoltaic (PV) systems, complemented by local biomass resources, which do not necessarily have to be pelletized. To investigate the configuration analysis, two operation systems (series and parallel) have been defined, represented by four different configurations. Firstly, these systems are compared to traditional monovalent configurations (heat pump only or the biomass boiler only) to determine if they improve the system's efficiency while minimizing operational costs and emissions. Secondly, the effect of layout and heat pump size is studied. Then, the effect of cut-off temperature on key parameters of the HHP system was investigated. Finally, defrosting was analyzed in terms of reduction in efficiency and additional cost. The optimum performance of the HHP system, in terms of energy efficiency, operational costs, and emissions, was depicted using a heat map diagram. The major results of the present study are highlighted as follows:

- In the choice of selecting an HHP or a monovalent system, the adequate configuration is the key to select an HHP as the best choice. According to the integrated efficiency, HHP series operation is consistently the best solution, and even further when a thermostatic valve is used to regulate the water flow between the heat pump and the boiler (i.e., configuration 2).
- Regarding the size of the HP in the HHP systems, the optimal performance depends on the configuration: in the serial HHP system, it is achieved with an 8 kW heat pump, while in the parallel system, the 4 kW heat pump outperforms the others.
- In all HHP configurations, the on–off cycles for heat pumps increase with the size of the heat pump. In contrast, the on–off cycles for biomass boilers generally decrease, with the exception of configuration 3 whose operation is more affected by the buffer tank.
- When examining environmental and economic KPIs, it is found that the HHP system is usually a better option than the monovalent system due to its combination of lower

emissions and reduced costs. Among all configurations, configuration 2 is again identified as the optimal choice.

- For each heat pump size, the seasonal energy performance improves with a higher cut-off temperature. As expected, this improvement comes from fewer defrost cycles and a shorter seasonal period during which the heat pump operates at a reduced COP because of the low temperatures.
- Increasing the cut-off temperature reduces the equivalent warming impact but raises the operational cost. This effect is likely due to the enhanced role of the biomass boiler in the HHP system.
- The defrosting effect is more pronounced in terms of efficiency, the number of on–off cycles, and additional costs with lower cut-off temperatures and a higher size of the HP in the HHP system.

For future work, it would be valuable to investigate the optimum heat pump size, cut-off temperature, and storage tank capacity, as well as their impact on the performance of the HHP system. Additionally, exploring the use of Phase Change Materials (PCMs) in the storage tank to support heat recovery during defrosting cycles could be an interesting area of study.

Author Contributions: Conceptualization, methodology, formal analysis, data curation, supervision, project administration, funding acquisition, validation, J.U.; formal analysis, software, investigation, writing—original draft preparation, M.T.J.; resources, writing—review and editing, A.M. All authors have read and agreed to the published version of the manuscript.

Funding: This research was funded by the TED2021-131397B-100 R&D project funded by MICIU/AEI/10.13039/501100011033/ and by the "European Union NextGenerationEU/PRTR".

Institutional Review Board Statement: Not applicable.

Informed Consent Statement: Not applicable.

Data Availability Statement: The raw data supporting the conclusions of this article will be made available by the authors on request.

Acknowledgments: The authors also give thanks to Ferroli España, S.L.U. Grupo Ferroli, for allowing us the use of their AWHP series in this research.

Conflicts of Interest: The authors declare no conflicts of interest.

References

1. Enker, R.A.; Morrison, G.M. Analysis of the transition effects of building codes and regulations on the emergence of a low carbon residential building sector. *Energy Build.* **2017**, *156*, 40–50. [CrossRef]
2. IEA. *Global Status Report for Buildings and Construction—Towards a Zero-Emissions, Efficient and Resilient Buildings and Construction Sector*; International Energy Agency: Paris, France, 2019.
3. Owrak, M.; Aminy, M.; Tajik Jamal-Abad, M.; Dehghan, M. Experiments and simulations on the thermal performance of a sunspace attached to a room including heat-storing porous bed and water tanks. *Build. Environ.* **2015**, *92*, 142–151. [CrossRef]
4. Tajik Jamal-Abad, M.; Saedodin, S.; Aminy, M. Heat transfer in concentrated solar air-heaters filled with a porous medium with radiation effects: A perturbation solution. *Renew. Energy* **2016**, *91*, 147–154. [CrossRef]
5. Tajik Jamal-Abad, M.; Saedodin, S.; Aminy, M. Variable conductivity in forced convection for a tube filled with porous media: A perturbation solution. *Ain Shams Eng. J.* **2018**, *9*, 689–696. [CrossRef]
6. Xu, W.; Liu, C.; Li, A.; Li, J.; Qiao, B. Feasibility and performance study on hybrid air source heat pump system for ultra-low energy building in severe cold region of China. *Renew. Energy* **2020**, *146*, 2124–2133. [CrossRef]
7. Klein, K.; Huchtemann, K.; Müller, D. Numerical study on hybrid heat pump systems in existing buildings. *Energy Build.* **2014**, *69*, 193–201. [CrossRef]
8. Xu, Y.; Guo, Z.; Yuan, C. Feasibility study of an integrated air source heat pump water heater/chillers and exhaust gas boiler heating system for swimming pool on luxury cruise ship. *Energy Rep.* **2022**, *8*, 1260–1282. [CrossRef]
9. Destro, N.; Benato, A.; Stoppato, A.; Mirandola, A. Components design and daily operation optimization of a hybrid system with energy storages. *Energy* **2016**, *117*, 569–577. [CrossRef]
10. Liu, C.; Han, W.; Wang, Z.; Zhang, N.; Kang, Q.; Liu, M. Proposal and assessment of a new solar space heating system by integrating an absorption-compression heat pump. *Appl. Energy* **2021**, *294*, 116966. [CrossRef]

11. Dongellini, M.; Naldi, C.; Morini, G.L. Sizing effects on the energy performance of reversible air-source heat pumps for office buildings. *Appl. Therm. Eng.* **2017**, *114*, 1073–1081. [CrossRef]
12. Park, H.; Nam, K.H.; Jang, G.H.; Kim, M.S. Performance investigation of heat pump-gas fired water heater hybrid system and its economic feasibility study. *Energy Build.* **2014**, *80*, 480–489. [CrossRef]
13. Chargui, R.; Sammouda, H. Modeling of a residential house coupled with a dual source heat pump using TRNSYS software. *Energy Convers. Manag.* **2014**, *81*, 384–399. [CrossRef]
14. Bellos, E.; Lykas, P.; Tzivanidis, C. Theoretical Analysis of a Biomass-Driven Single-Effect Absorption Heat Pump for Heating and Cooling Purposes. *Appl. Syst. Innov.* **2022**, *5*, 99. [CrossRef]
15. Li, G. Parallel loop configuration for hybrid heat pump—Gas fired water heater system with smart control strategy. *Appl. Therm. Eng.* **2018**, *138*, 807–818. [CrossRef]
16. Keogh, D.; Saffari, M.; de Rosa, M.; Finn, D.P. Energy assessment of hybrid heat pump systems as a retrofit measure in residential housing stock. In *E3S Web of Conferences*; EDP Sciences: Les Ulis, France, 2019; p. 01064. [CrossRef]
17. Bagarella, G.; Lazzarin, R.; Noro, M. Annual simulation, energy and economic analysis of hybrid heat pump systems for residential buildings. *Appl. Therm. Eng.* **2016**, *99*, 485–494. [CrossRef]
18. Bennett, G.; Watson, S.; Wilson, G.; Oreszczyn, T. Domestic heating with compact combination hybrids (gas boiler and heat pump): A simple English stock model of different heating system scenarios. *Build. Serv. Eng. Res. Technol.* **2022**, *43*, 143–159. [CrossRef]
19. Fischer, D.; Lindberg, K.B.; Madani, H.; Wittwer, C. Impact of PV and variable prices on optimal system sizing for heat pumps and thermal storage. *Energy Build.* **2016**, *128*, 723–733. [CrossRef]
20. Di Perna, C.; Magri, G.; Giuliani, G.; Serenelli, G. Experimental assessment and dynamic analysis of a hybrid generator composed of an air source heat pump coupled with a condensing gas boiler in a residential building. *Appl. Therm. Eng.* **2015**, *76*, 86–97. [CrossRef]
21. Sun, M.; Djapic, P.; Aunedi, M.; Pudjianto, D.; Strbac, G. Benefits of smart control of hybrid heat pumps: An analysis of field trial data. *Appl. Energy* **2019**, *247*, 525–536. [CrossRef]
22. D'Ettorre, F.; Conti, P.; Schito, E.; Testi, D. Model predictive control of a hybrid heat pump system and impact of the prediction horizon on cost-saving potential and optimal storage capacity. *Appl. Therm. Eng.* **2019**, *148*, 524–535. [CrossRef]
23. Martínez-Gracia, A.; Usón, S.; Pintanel, M.T.; Uche, J.; Bayod-Rújula, Á.A.; Del Amo, A. Exergy assessment and thermo-economic analysis of hybrid solar systems with seasonal storage and heat pump coupling in the social housing sector in Zaragoza. *Energies* **2021**, *14*, 1279. [CrossRef]
24. Martínez-Gracia, A.; Uche, J.; Del Amo, A. Energy and environmental benefits of an integrated solar photovoltaic and thermal hybrid, seasonal storage and heat pump system for social housing. *Appl. Therm. Eng.* **2022**, *213*, 118662. [CrossRef]
25. Menberg, K.; Heo, Y.; Choi, W.; Ooka, R.; Choudhary, R.; Shukuya, M. Exergy analysis of a hybrid ground-source heat pump system. *Appl. Energy* **2017**, *204*, 31–46. [CrossRef]
26. Lee, C.G.; Cho, L.H.; Park, S.; Kim, S.J.; Jeong, I.S.; Kim, M.J.; Kim, D.H. Smart farm heating using a hybrid pellet boiler–hydrothermal heat pump system. *J. Biosyst. Eng.* **2022**, *47*, 233–247. [CrossRef]
27. Guntamatic. Hybrid: Pellet Heat Pump. Available online: https://www.guntamatic.com/en/products/hybrid/pellet-heat-pump/hybrid-010016/ (accessed on 9 October 2024).
28. Hargassner. Hybrid Heat Pump. Available online: https://www.hargassner.com/at-en/hybrid-heat-pump/ (accessed on 9 October 2024).
29. Klein, S.A.; Beckman, W.A.; Mitchell, J.W. *TRNSYS 18: A Transient System Simulation Program*; Solar Energy Laboratory, University of Wisconsin: Madison, WI, USA, 2019.
30. Dongellini, M.; Morini, G.L. On-off cycling losses of reversible air-to-water heat pump systems as a function of the unit power modulation capacity. *Energy Convers. Manag.* **2019**, *196*, 966–978. [CrossRef]
31. Bagarella, G.; Lazzarin, R.; Noro, M. Sizing strategy of on-off and modulating heat pump systems based on annual energy analysis. *Int. J. Refrig.* **2016**, *65*, 183–193. [CrossRef]
32. Minglu, Q.; Liang, X.; Deng, S.; Yiqiang, J. A study of the reverse cycle defrosting performance on a multi-circuit outdoor coil unit in an air source heat pump—Part I: Experiments. *Appl. Energy* **2012**, *91*, 122–129. [CrossRef]
33. *BOE no. 253, 22/10/1979*; Royal Decree 2429/1979, of July 8th, Approves the Basic Building Standard NBECT-79 on Building Thermal Conditions. Spanish Government: Madrid, Spain, 1979.
34. *BOE no. 311, 27/12/2019*; Royal Decree 732/2019, of December 20th, Which Modifies the Technical Building Code, Approved by Royal Decree 314/2006, of March 17th. Spanish Ministry of Development: Madrid, Spain, 2019.
35. Ministerio de Industria; Energía y Turismo; Ministerio de Fomento. *Factores de Emisión de CO_2 y Coeficientes de Paso a Energía Primaria de Diferentes Fuentes de Energía Final Consumidas en el Sector de Edificios en España*; Spanish Government: Madrid, Spain, 2014.
36. *Standard EN 14825:2016*; Air Conditioners, Liquid Chilling Packages and Heat Pumps, with Electrically Driven Compressors, for Space Heating and Cooling—Testing and Rating at Part Load Conditions and Calculation of Seasonal Performance. European Committee for Standardization (CEN): Brussels, Belgium, 2016.

37. Malenković, I.; Pärisch, P.; Eicher, S.; Bony, J.; Hartl, M. Definition of Main System Boundaries and Performance Figures for Reporting on SHP Systems: Deliverable B1. International Energy Agency, SHC Task 44/HPP Annex 38. Available online: https://task44.iea-shc.org/publications (accessed on 21 October 2024).
38. Ecoinvent Association. Ecoinvent Database 3.6, Cut-Off. Available online: www.ecoinvent.org (accessed on 21 October 2024).
39. Red Eléctrica de España. Hourly Prices for Electricity in Spain. *Daily Downloadable Files.* Available online: https://www.esios.ree.es/es/descargas (accessed on 21 October 2024).
40. Dongellini, M.; Naldi, C.; Morini, G.L. Influence of sizing strategy and control rules on the energy saving potential of heat pump hybrid systems in a residential building. *Energy Convers. Manag.* **2021**, *235*, 114129. [CrossRef]
41. Beccali, M.; Bonomolo, M.; Martorana, F.; Catrini, P.; Buscemi, A. Electrical hybrid heat pumps assisted by natural gas boilers: A review. *Appl. Energy* **2022**, *322*, 119466. [CrossRef]
42. Madonna, F.; Bazzocchi, F. Annual performances of reversible air-to-water heat pumps in small residential buildings. *Energy Build.* **2013**, *65*, 299–309. [CrossRef]
43. Rossi di Schio, E.; Ballerini, V.; Dongellini, M.; Valdiserri, P. Defrosting of Air-Source Heat Pumps: Effect of Real Temperature Data on Seasonal Energy Performance for Different Locations in Italy. *Appl. Sci.* **2021**, *11*, 8003. [CrossRef]